JOURNAL OF AIRCRAFT
Vol. 30, No. 5, Sept.–Oct. 1993

Ground Facility Interference on Aircraft Configurations with Separated Flow

M. E. Beyers*
Institute for Aerospace Research, Ottawa, Ontario, Canada
and
L. E. Ericsson†
Lockheed Missiles and Space Company, Inc., Sunnyvale, California 94088

Analysis of recent test results obtained on strut-mounted aircraft models has revealed the presence of test facility interference effects. In addition to dynamic support interference, coupling with unsteady wall interference effects can be present even when the model is relatively small in relation to the test section size. This coupled support/wall interference is expected to be more prevalent in pitch-oscillation than in roll-oscillation tests. Significant interference of this type was identified in dynamic cross-coupling data obtained on the standard dynamics model (SDM) oscillating in pitch. On the other hand, small distortions of the antisymmetrical static rolling moment characteristics and of the longitudinal aerodynamic characteristics measured on a 65-deg delta wing are shown to be attributable to the effect of direct support interference on vortex breakdown. For the oscillating delta wing, the support interference produces asymmetries in the measured longitudinal aerodynamic characteristics, which decrease with increasing roll rate.

Nomenclature

b = wingspan
b_s = span of rotor arm
C = aerodynamic coefficient; with no superscript, in body axes system
C_{ij} = $\partial C_i/\partial(j\bar{c}/2V)$, $i = l, m, n$; $j = q, q', \dot{\alpha}, \dot{\sigma}$
C_{ik} = $\partial C_i/\partial k$, $i = l, m, n$; $k = \alpha, \beta, \sigma$
C_l = rolling moment coefficient, $M_x/(q_\infty Sb)$
C_m = pitching moment coefficient, $M_y/(q_\infty S\bar{c})$
C_N = normal force coefficient, $N/(q_\infty S)$
C_n = yawing moment coefficient, $M_z/(q_\infty Sb)$
C_p = static pressure coefficient, $(p_s - p_\infty)/q_\infty$
C_{yf} = fin side-force coefficient
c = $\bar{c}/b$
$\bar{c}$ = mean aerodynamic chord
M_x, M_y, M_z = rolling, pitching, and yawing moments about x, y, and z, Fig. 3
M_∞ = freestream Mach number
p, q, r = body axes angular velocities
p_s = local static pressure
p_∞ = freestream static pressure
q' = aerodynamic axes pitch rate
q_∞ = freestream dynamic pressure
S = reference area
V = freestream velocity
w = minimum dimension of test section
X, Y, Z = wind axes system
x_t = longitudinal tunnel coordinate
x, y, z = body axes system
x', y', z' = aerodynamic axes system
y_s = location of support strut, Fig. 8
y_0 = test section dimension, Fig. 8
α, β = angles of attack and sideslip
Δ = increment or amplitude
Δt_v = vortex formation time lag
Δt_{vs} = convective time lag associated with support interference
δ_s = sting deflection, Fig. 6
$\sigma, \hat{\phi}$ = total angle of attack and bank angle
ϕ = roll angle
ϕ' = roll orientation angle of model symmetry plane
ω = angular frequency
$\bar{\omega}, k$ = reduced circular frequency, $\omega d/(2V)$ where $d = \bar{c}$ or b

Superscripts
$\cdot$ = differentiation with respect to time
$\hat{}$ = aerodynamic axes system
$\tilde{}$ = oscillatory condition

Introduction

MODEL support system interference is an area of concern in aerodynamic experiments, particularly at high incidence, where disturbances to the leeside vortical flow occur. In the past, the interaction between the vortices shed from slender forebodies at high angles of attack and a downstream support has received the most attention.[1,2] However, subsonic experimental results published later for the standard dynamics model (SDM)[3] show that when the model is side-mounted,[4] a similar problem is presented by the interaction between the leading-edge vortices shed from slender wings and the downstream support[5] (Fig. 1).

For relatively large models ($b/w \geq 0.6$) the support interference can be coupled with unsteady wall interference effects.[5] In this case, the leeside vortex system is influenced by effects communicated from the walls directly, as well as by way of the support. To determine to what extent this complex form of ground test interference depends on the (relative) model size, the interference flowfield around a strut-mounted SDM was investigated in a larger wind tunnel.[6] In large-amplitude, high-rate roll oscillation tests of a sharp-edged 65-deg delta wing, performed earlier in this tunnel using the same support system,[7] the support interference had been found to

Presented as Paper 92-0673 at the AIAA 30th Aerospace Sciences Meeting, Reno, NV, Jan. 1992; received Feb. 13, 1992; revision received July 20, 1992; accepted for publication July 21, 1992.

*Senior Research Officer, Applied Aerodynamics Laboratory. Member AIAA
†Engineering Consultant. Fellow AIAA

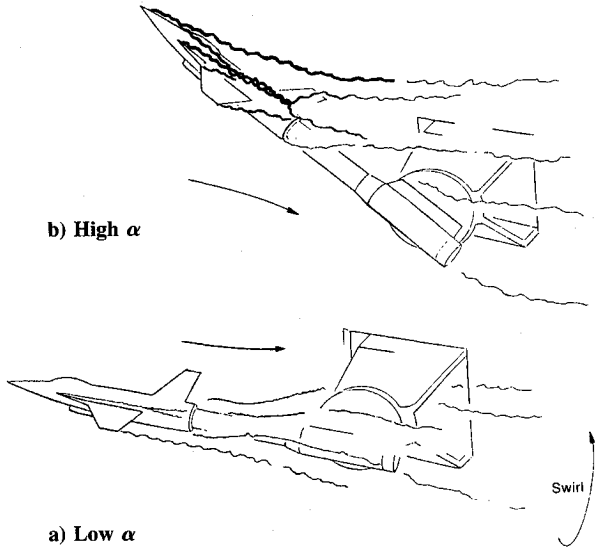

Fig. 1 Aircraft model on sidewall support system.[5]

vary greatly with the oscillation frequency, decreasing with increasing frequency.[8]

In this article the conditions under which coupled support/wall interference can arise are explored, providing insight into the nature of the flow phenomena involved in both roll- and pitch-oscillation experiments. The present analysis of two different strut support systems should provide some answers which could be useful when considering other experimental installations.[9]

Pitch-Oscillation Experiment

The sidewall support system depicted in Fig. 1 was used to investigate dynamic cross-coupling effects on the SDM.[3] The A-frame support[4] (Fig. 2) was mounted on the reflection plane of an asymmetrical test section, opposed by a slotted wall. The model was banked at an angle $\hat{\phi}$ and oscillated at an amplitude of ± 1 deg about the aerodynamic pitch axis. The reference systems are shown in Fig. 3. When the angle between the symmetry planes of the model and the tunnel, $\phi' = \hat{\phi} + n\pi$ where $n = 0, 1$, was varied, the results shown in Fig. 4 were obtained.

At $\beta = 0$ ($\hat{\phi} = 0$) and $\alpha \leq 10$ deg the measured mean $C_{lq} + C_{l\dot{\alpha}}$ is near zero,[3] as expected. The unsteady interference contributions were found to be negligible at $\alpha = 0$ deg, and small but measurable at $\alpha = 10$ deg (of the order of the experimental uncertainty). At $\phi' = 0$ and 180 deg, the wing trailing edge is lined up with the pitch axis of the support, resulting in roughly equal and opposite interference contributions. The opposition between the static and dynamic derivatives is the expected manifestation of a convective flowfield time lag.[1,2]

When the cross-coupling derivatives $\hat{C}_{lq'} + \hat{C}_{l\dot{\sigma}}$ and $\hat{C}_{nq'} + \hat{C}_{n\dot{\sigma}}$ are determined at nonzero bank angles, a more complete picture emerges. The results obtained at four orientations giving $\alpha = 10$ deg and $\beta = \pm 5$ deg are correlated with ϕ' in Figs. 4 and 5. The asymmetrical variations in both sets of cross-coupling derivatives are now large, indicating that the wing wake is sharply deflected by disturbances in the flowfield. The simple time-lag opposition of static and dynamic interference effects found in the rolling moment derivatives (Fig. 4) is absent in Fig. 5, indicating that the flow mechanism causing the effects on $\hat{C}_{nq'} + \hat{C}_{n\dot{\sigma}}$ and $\hat{C}_{n\sigma}$ is more complex than that associated with direct support interference. In particular, direct interaction of the fin with the strut does not appear to constitute a dominant source of interference here; measurements at each of two geometrical mirror image positions yielded larger differences in the dynamic yawing moment derivative with the fin directed away from ($\phi' = 27$ and 153 deg) rather than towards the A-frame strut ($\phi' = 207$

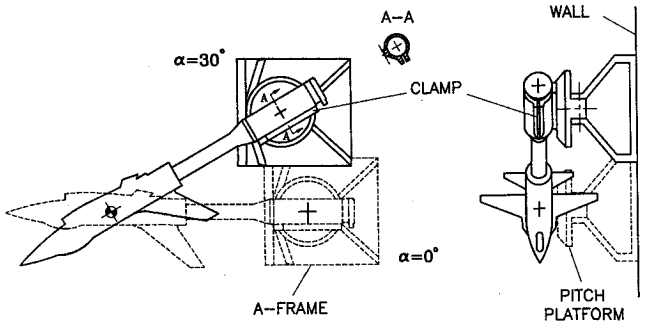

Fig. 2 Geometrical details of sidewall support system.[4]

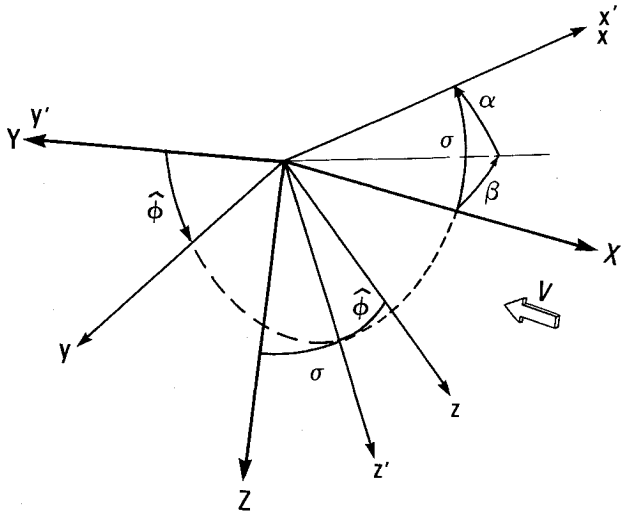

Fig. 3 Reference systems.[3]

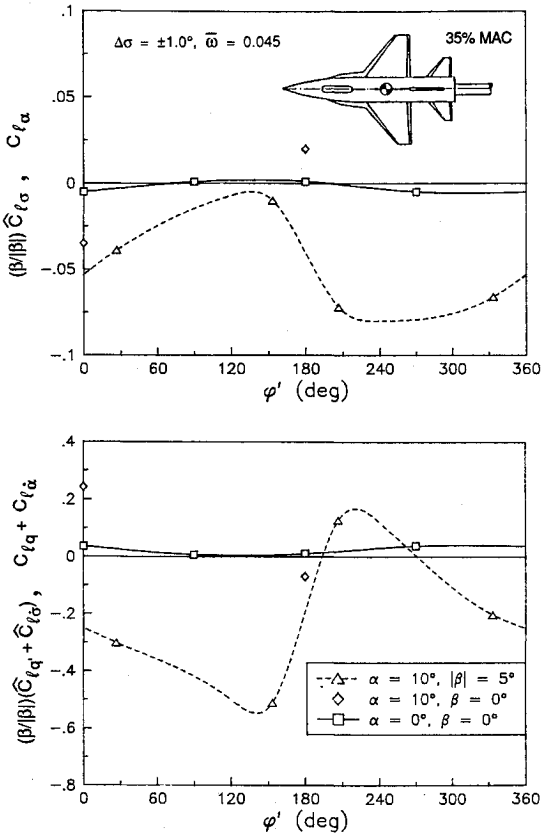

Fig. 4 Effect of model roll orientation on SDM rolling moment derivatives at $M_\infty = 0.6$.[5]

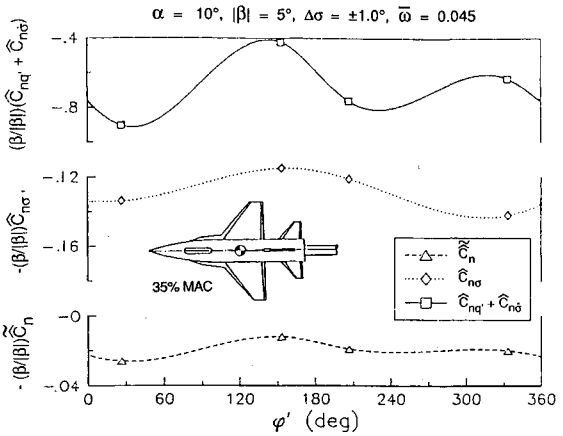

Fig. 5 Effect of model roll orientation on SDM yawing moment derivatives at $M_\infty = 0.6$.[5]

and 333 deg) (Fig. 5). Therefore, these asymmetries are identified with changes in the orientation of the model relative to the test section symmetry plane.

On the other hand, the largest changes in the rolling moment derivatives occur between the orientations with the fin directed upward, as in Fig. 1, rather than towards the support. The reason for the essentially discontinuous change in $\hat{C}_{lq'} + \hat{C}_{l\dot{\sigma}}$ occurring when ϕ' is increased from 153 to 207 deg can be understood with reference to the strut geometry[4] shown in Fig. 2. The sting is held in a split cylinder, integral with the pitch platform and incorporating a clamp on the upper side. In the "normal" condition, for positive pitch angles, depicted in Fig. 2, the wake encounters the smooth side of the sting base by design. In contrast, for the negative pitch angles associated with the $\phi' = 153$- and 207-deg attitudes, the swirling wake is deflected by the longitudinal flat surfaces of the sting clamp.

In this condition, the wing wake interacts with these surfaces in a manner reminiscent of the interaction of a slender-body wake with a sting support discussed in Ref. 1. The effect of δ_s had been found to be highly nonlinear, with a more or less discontinuous C_m change between $\delta_s = 0$ and -1 deg (see Fig. 6). As the sting is pitched to the windward side, $\delta_s < 0$, its leeward side becomes more deeply submerged in low-energy wake flow. The windward side reattachment pressure increases relative to the leeward side until, through the upstream communication, it flips the wake to the leeward side. Therefore, a negative base load and a discontinuous, statically destabilizing increase in the pitching moment result.

In the present case, the deflection of the wing wake by the clamp mechanism (and the pitch platform) is influenced by the flowfield fluctuations communicated from the slotted wall. The smaller differences between the data at $\phi' = 27$ deg and $\phi' = 333$ deg suggest a dependence on the orientation with respect to the slotted wall, and possible coupling with unsteady wall effects. On the other hand, this might be attributed to the presence of the pitch platform (Fig. 2). In either case, the effects on $\hat{C}_{lq'} + \hat{C}_{l\dot{\sigma}}$ and $\hat{C}_{l\sigma}$ are dominated by communication between the wing and the support, giving the single time lag effects seen in Fig. 4. The type of support interference caused by the clamp mechanism is of interest, but it should be noted that this is not present in normal tests with this installation, where $\sigma > 0$ and -90 deg $\leq \phi' \leq 90$ deg.

As already noted, the behavior is more complex in the case of the yawing moment derivatives. In Ref. 5 it was shown that the existence of an unsteady, coupled support/wall interference phenomenon is consistent with the observations in Fig. 5. Wall static pressure measurements showed that pressure disturbances due to flow through the plenum chamber induced by wake blockage of the model and support, extend across the entire test section. Upstream of the model, the flow

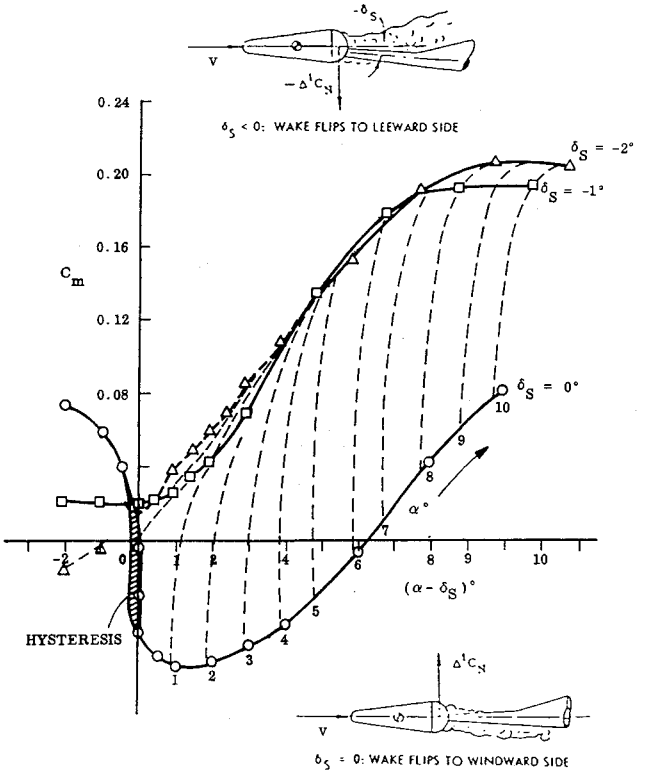

Fig. 6 Pitching moment carpet plot for $M_\infty = 0.26$.[1]

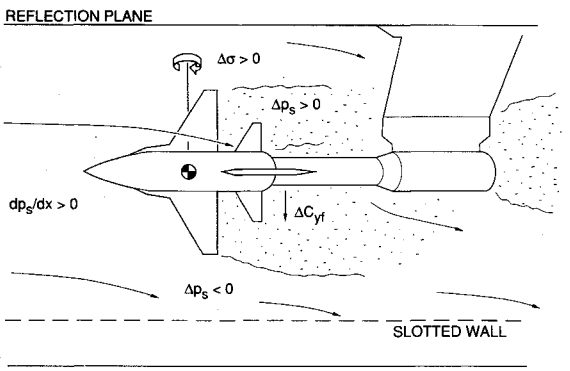

Fig. 7 Flow response to pitch change at medium α.[5]

deflection is thought to be two-dimensional (see Fig. 7), giving way to swirling flow between the model and the strut (see Fig. 1). For the oscillating model, the fluctuating wake blockage causes periodic deflections of the upstream flowfield and of disturbances emanating from the slotted wall, perturbing the nonplanar flow around the strut synchronously with the model motion. Thus, the yawing-moment derivatives $\hat{C}_{nq'} + \hat{C}_{n\dot{\sigma}}$ and $\hat{C}_{n\sigma}$ are seen to be influenced not only by the flowfield time lag associated with the fluctuating upstream two-dimensional flow but also by a second convective time lag, associated with communication between the model and the plenum and back to the model by way of the support.

Strut Interference Flowfield

In rotary balance tests, coupled support/wall interference was found to be present[5] at a ratio $b_s/w = 0.6$, but not at a ratio of 0.4 where support interference due to steady deflection of the vortex wake[2] was still present. In both cases, the distortions of the experimental data were significant. Another investigation was made[6] to determine whether oscillatory tests in a 2 × 3 m low-speed wind tunnel would also be subject to coupled support/wall interference effects. In this case, the SDM was tested at a scale giving $b/w = 0.32$.

Simple strut interference may be expected to exist in the absence of unsteady wall effects. For an asymmetrical strut, such as that depicted in Fig. 8, a particular type of support interference exists. This does not mean that for a symmetrical support system there is no support interference; only that in the latter case the interference is more difficult to detect since its blockage effects are symmetrical relative to the $\beta = 0$ condition.

The nature of the flow asymmetry arising from the asymmetrical blockage presented by the strut was revealed through smoke flow visualization.[6] Figure 9 is a composite of identical views from two tests at $\sigma = 21.4$ deg ($\alpha = 19$ deg), with the model banked at $\hat{\phi} = 28.4$ and -28.4 deg, respectively ($\beta = \pm 10$ deg). The smoke trails were symmetrically positioned below the windward strakes in the two cases. Since the horizontal projections of the smoke trajectories would be identical in the absence of any flowfield disturbance, the divergence of the smoke trails is attributed to interference caused by the strut and, possibly, the walls. Combination of these displacements with the corresponding vertical plane displacements showed that a sharp rotation of the plane of the flow deflection had occurred downstream of the model. At $\sigma = 29.6$ deg the flow deflections were similar, albeit further to the side of the strut.

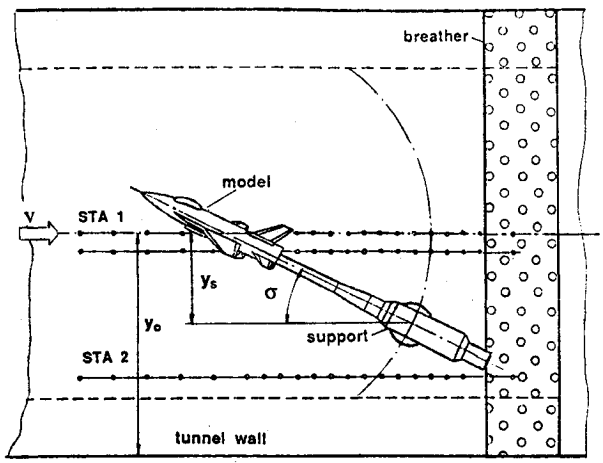

Fig. 8 Asymmetrical support installation in 2 × 3 m low-speed wind tunnel.[6]

Fig. 9 Composite view of smoke flow visualization at positive and negative bank angles $\hat{\phi} = \pm 28.4$ deg, $\sigma = 21.4$ deg.[6]

The strut-induced nonuniformities in the pressure distribution accompanying these angularities were equally pronounced. Consider the case of $\beta = 0$ deg at $\alpha = 28$ deg. Figures 10a and 10b contain the streamwise floor static pressure signatures along the tunnel centerline (STA 1), in line with the model reference center, and near the wall closest to the strut (STA 2). The results show that the potential for strut interference exists even at a relatively large angle of attack of $\alpha = 28$ deg, where the vortex wake from the SDM passes above and to the side of the strut support. While the obstruction presented by this support appears to be more benign than that of the obstacle used in Hummel's classical experiment[10] (Fig. 11), the strong pressure gradients around the asymmetrical strut may nevertheless be expected to influence vortex breakdown and, in particular, cause asymmetrical breakdown.

The immediate question here is whether or not the support interference effects on an oscillating model are coupled with unsteady wall interference effects. Figure 10 shows that at β

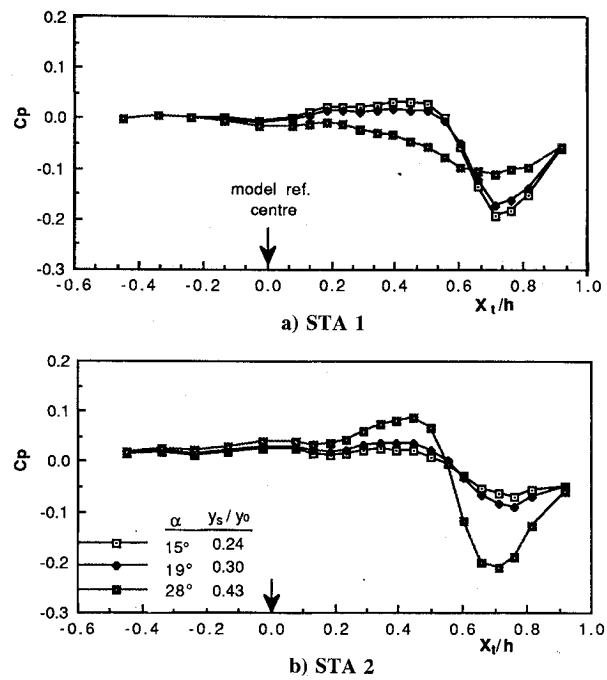

Fig. 10 Static pressure signatures at zero sideslip.[6]

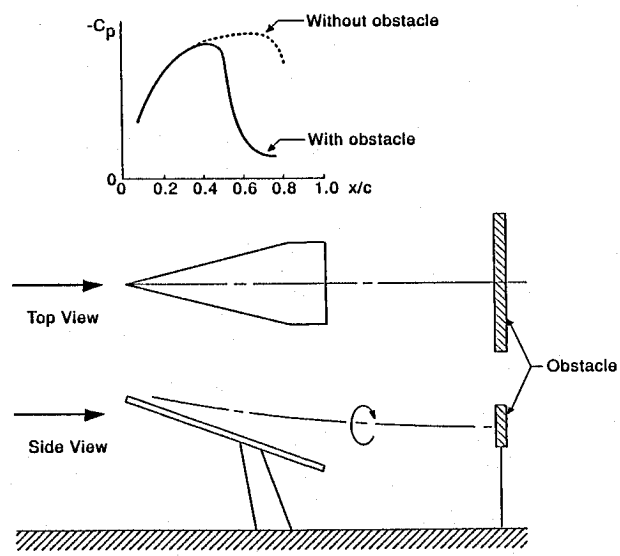

Fig. 11 Vortex breakdown on a 75-deg delta wing caused by downstream obstacle.[10]

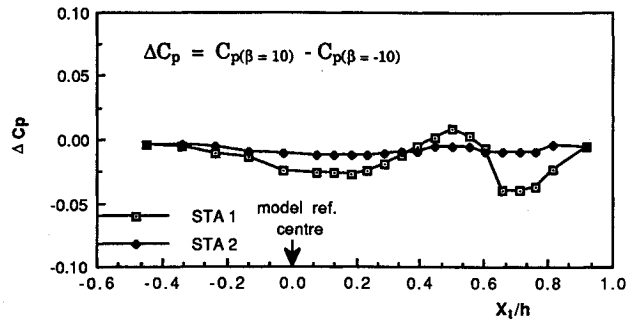

Fig. 12 Static pressure increment for symmetrical roll deflections at $\alpha = 28$ deg.[6]

$= 0$ and low incidence angles ($\alpha \leq 19$ deg) the strut blockage effect in the region just downstream of the model is appreciable, but the effect of the presence of the model is small.[6] On the other hand, the wake blockage effect of the model is clearly significant at $\alpha = 28$ deg, when massive separation is present. At the far side of the strut (STA 2) the pressure drop due to model wake blockage is less evident, but the pressure rise due to strut blockage is very pronounced at the higher incidence angle. Thus, both static support and wall interference effects are present at high α ($\alpha \geq 28$ deg).

For the nonsymmetrical case, the pressure distributions were examined for $\beta = \pm 10$ deg ($\sigma = 29.6$ deg). The blockage contributions are similar to those for $\beta = 0$, but the effects of asymmetry are of particular interest. As shown in Fig. 12, the increment in the pressure coefficient, $\Delta C_p = C_{p(\beta=10)} - C_{p(\beta=-10)}$, is significant at the tunnel centerline, but small at the far side of the strut. That is, the pressure changes are felt along the floor beneath the model but not further afield, suggesting that they are mainly due to the change in downwash direction between $\beta = 10$ and -10 deg.

Pitch oscillations of an aircraft model at high incidence are accompanied by fluctuating wake blockage (Fig. 7). The resulting pressure disturbances will be reflected from the walls, introducing the possibility of unsteady coupling with the support interference mechanism. On the other hand, for an aircraft model oscillating in roll, σ is constant and the magnitude of the wake blockage remains essentially unchanged except at very large roll angles. Thus, coupled support/wall interference could be significant in pitch oscillation tests, even for the model size giving $b/w = 0.32$ (Fig. 8). However, it is considered unlikely in roll oscillation tests at amplitudes below $\Delta\phi = \pm 20$ deg, where direct support interference is expected to prevail.

Roll-Oscillation Tests

Large-amplitude, high-rate oscillations in roll of a sharp-edged 65-deg delta wing (Fig. 13) were performed[7] with the same support used later in the SDM experiment.[6] Figure 14 shows the asymmetrical blockage presented to the vortex wake of the delta wing model. This model is not as slender as the SDM forebody/strake configuration, but the proportions ($b/w = 0.30$) and wing area, and, therefore, the wake blockage, are roughly similar. Thus, under the same test conditions, the 65-deg delta wing and the SDM could be expected to produce similar disturbances and to experience support interference of the same type.

According to flow visualization results[8] at $\sigma = 30$ deg, the support strut causes asymmetrical vortex breakdown even at $\phi = 0$. The deflection of the vortex system would be similar to that in Fig. 9, suggesting that a locally increased adverse pressure gradient caused the observed early vortex breakdown on the starboard wing-half. Further downstream, a favorable pressure gradient develops as indicated by the pressure distribution for $\alpha = 28$ deg in Fig. 10a. For a positive roll angle, $\phi > 0$, the deflection of the vortex wake from the windward, starboard wing is amplified by support interference

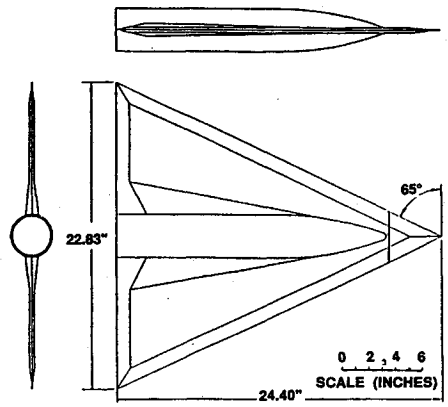

Fig. 13 Delta wing model.[7]

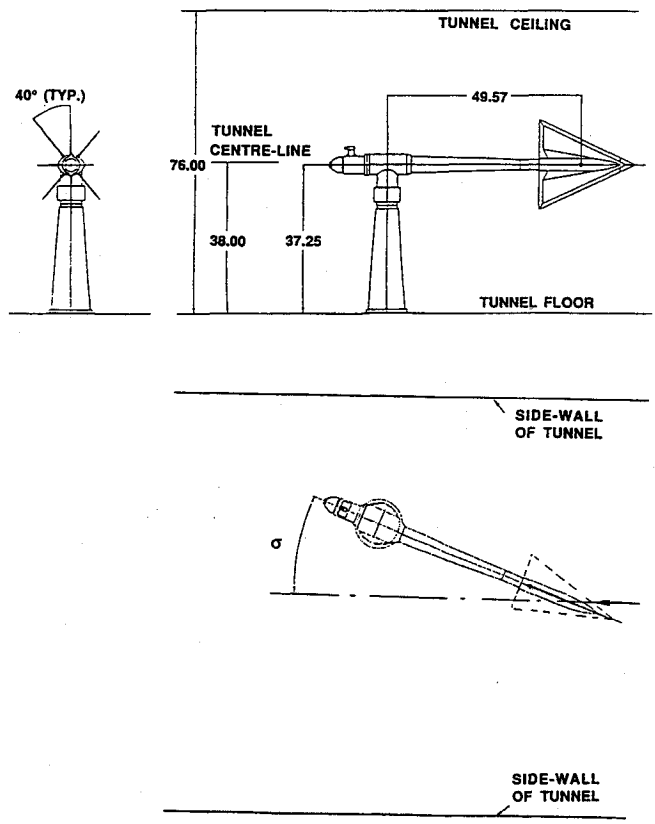

Fig. 14 Support system for tests of 65-deg delta wing model.[11]

(Fig. 9), and vortex breakdown will occur earlier than for the port-side wing at $\phi < 0$, where the support interference should be smaller. This is in agreement with the asymmetry exhibited by the static $C_N(\phi)$ characteristics[11] (Fig. 15), which show lower C_N values for positive than for negative roll angles of the same magnitude.

Rolling Moment Characteristics

The $C_l(\phi)$ results[12] in Fig. 16 show that the starboard wing experiences support interference also when it is on the leeward side, at $\phi < 0$. As discussed in detail in Ref. 12, the statically destabilizing data trend is caused by the vortex breakdown leaving the leeward wing. The data in Fig. 16 indicate that this occurrence is delayed when the leeside wing (in the lateral sense) is located in the lower half of the test section, where the support interference has the largest effect on vortex breakdown (see Fig. 14). The fast downstream movement of vortex breakdown started at $\phi > 2$ deg, when the port-side wing was the leeward one, but not until $\phi < -5$ deg when the starboard wing was on the leeside. Thus, in this case, the support in-

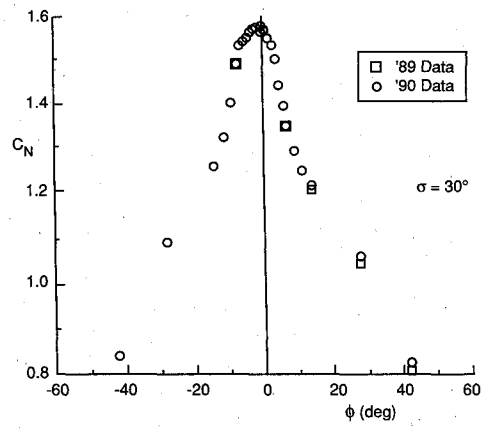

Fig. 15 Static $C_N(\phi)$ characteristics of 65-deg delta wing.[11]

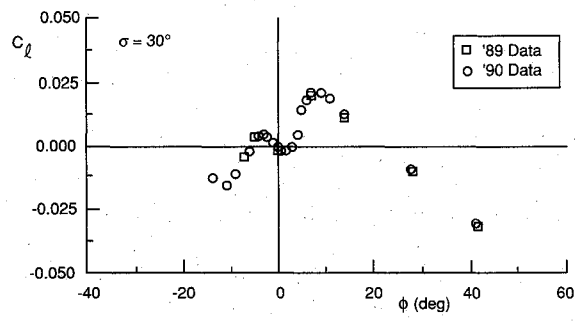

Fig. 16 Static $C_l(\phi)$ characteristics of 65-deg delta wing.[12]

terference decreases the normal force on the starboard wing both for $\phi > 0$ and $\phi < 0$. The asymmetrical $C_N(\phi)$ characteristics in Fig. 15 are consistent with the fact that the support interference on the starboard wing is largest at $\phi > 0$, when it is on the windward side. In regard to the $C_l(\phi)$ characteristics,[12] the support interference is statically destabilizing for $\phi > 0$, when the windward wing experiences the full burst-promoting effect of the support. However, when $\phi < 0$, the support-induced effect on the leeward wing delays the downstream travel of the vortex breakdown, a statically stabilizing effect. At $\sigma = 30$ deg, this strong effect is limited to the range -10 deg $< \phi < 10$ deg, where it results in a statically destabilizing slope that is larger for 2 deg $< \phi < 10$ deg than for -10 deg $< \phi < -5$ deg (Fig. 16).

Dynamic Test Results

In the dynamic tests performed on the 65-deg delta wing at $\sigma = 30$ deg, the dynamic $C_l(\phi)$ loops obtained do not exhibit any clear asymmetries.[11,13] This is surprising in view of the well-defined effect of support interference found in the static $C_l(\phi)$ and $C_N(\phi)$ characteristics. The roll-rate-induced camber delays vortex breakdown on the downstroke, and promotes breakdown on the upstroke.[13,14] Thus, for oscillations around $\phi = 0$, vortex breakdown does not leave the leeward wing for the range of reduced roll rate tested, $0.08 \leq |\dot{\phi}b/2V| \leq 0.20$. On the downstroke of the windward wing half, i.e., on the starboard side for $\phi > 0$ and $\dot{\phi} > 0$, the camber effect creates a cohesive leading-edge vortex that, even after spiral vortex breakdown, could result in a vortex wake of rather modest cross section, causing the support interference to be smaller than in the static test.

In addition to this roll-rate effect, one has to consider the time lag Δt_{vs} that occurs before the support interference effect results in a change in the aerodynamic loads on the model. When adding this time lag to the time lag associated with the vortex formation over the delta wing,[13,14] Δt_v, the resulting total phase lag can be large. Thus, during the "backstroke" ($\phi > 0$, $\dot{\phi} < 0$), the starboard wing may never experience the increased support interference associated with the reverse

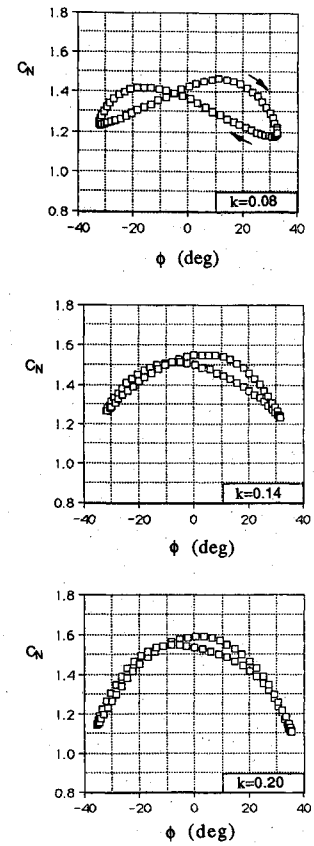

Fig. 17 Dynamic $C_N(\phi)$ loops around $\phi = 0$ for 65-deg delta wing at $\Delta\phi = 33$ deg.[11]

camber effect generated during the backstroke, and instead experience the support interference generated during the "downstroke" a time increment ($\Delta t_v + \Delta t_{vs}$) earlier. This would explain the undistorted appearance of the $C_l(\phi)$ loops.[11,13] Why the dynamic $C_N(\phi)$ loops show such distinct asymmetry, especially at low frequencies[11] (Fig. 17) still remains to be explained.

In the absence of support interference, the starboard and port sides of the delta wing would balance each other for each half cycle, $-\Delta\phi < \phi \leq 0$, $0 \leq \phi < \Delta\phi$, etc. Looking at the $C_N(\phi)$ loops for $k = 0.20$ in Fig. 17, one finds that the up- and downstroke branches almost coincide, as would be expected in the absence of support interference. The absence of similar characteristics for $k = 0.14$ and $k = 0.08$ indicates that in these cases the support interference has a significant effect.

The reasons for the decreasing support interference with increasing k are the roll-rate induced camber effect discussed earlier, and the associated increasing phase lag. At $k = 0.08$, this phase lag apparently is such that the roll-rate-induced camber effect lasts a little past the end of the downstroke, up to perhaps $\phi = 20$ deg. The minimum C_N is realized on the backstroke, when the support interference generated during the downstroke reaches the delta wing surface. Applying the same phase lag during the backstroke, the more severe support interference associated with it will not reach the model until $\phi < 0$, explaining the lower peak value of $C_N(\phi)$ for $\phi < 0$ compared to $\phi > 0$. As k is increased, the realization of support interference is further delayed. Thus, it appears that $k = 0.14$, the smaller support interference associated with the downstroke is realized during the backstroke, raising this part of the $C_N(\phi)$ loop (for $\phi < 20$ deg and $\dot{\phi} < 0$ in Fig. 17). Finally, at $k = 0.20$, the increased phase lag has apparently delayed the arrival at the model of the support interference effect so much that the starboard wing has had time to reach the leeside when this occurs.

Conclusions

Experimental results have been analyzed to determine the conditions under which simple support interference and coupled support/wall interference can occur in dynamic tests. The results can be summarized as follows:

1) The effects of coupling between support and wall interference are likely to be larger in pitch oscillation than in roll oscillation tests.

2) The interference effects observed in the SDM experiments may be attributed to direct support interference on the rolling moment derivatives and coupled support/wall interference on the yawing moment derivatives.

3) Direct support interference on vortex breakdown appears to be the primary source of the observed interference effects in the roll oscillation tests of a 65-deg delta wing at high incidence.

4) The support interference effect on vortex breakdown is strongly dependent on the reduced roll rate through the roll-rate-induced camber effect on the leading-edge vortices, and through the associated convective time lag effect.

The interference results analyzed were obtained on asymmetrically mounted models; however, this type of interference is not restricted to asymmetrical supports, although it is easier to detect for an asymmetrical than for a symmetrical support system. More experimentation and analysis will be needed before this complicated flow phenomenon will be fully understood.

References

[1]Ericsson, L. E., and Reding, J. P., "Review of Support Interference in Dynamic Tests," *AIAA Journal*, Vol. 21, No. 12, 1983, pp. 1652–1666.

[2]Ericsson, L. E., and Reding, J. P., "Dynamic Support Interference in High Alpha Testing," *Journal of Aircraft*, Vol. 23, No. 12, 1986, pp. 889–896.

[3]Beyers, M. E., "SDM Pitch- and Yaw-Axis Stability Derivatives," AIAA Paper 85-1827, Aug. 1985.

[4]Beyers, M. E., "Some Recent Experiences of Support Interference in Dynamic Tests," National Research Council (Canada), NAE-LTR-UA-83, Ottawa, Canada, Nov. 1985.

[5]Beyers, M. E., "Unsteady Wind-Tunnel Interference in Aircraft Dynamic Experiments," *Journal of Aircraft*, Vol. 29, No. 6, 1992, pp. 1122–1129.

[6]Beyers, M. E., Cai, H. J., and Penna, P. J., "Flow-Field Interference Produced by an Asymmetrical Support Strut," National Research Council (Canada), IAR-AN-75, Ottawa, Canada, Jan. 1993.

[7]Hanff, E. S., and Jenkins, S. B., "Large-Amplitude High-Rate Roll Experiments on Delta and Double Delta Wing," AIAA Paper 90-0224, Jan. 1990.

[8]Hanff, E. S., private communication, Ottawa, Canada, April 1991.

[9]Johnson, J. L., Jr., Grafton, S. B., and Yip, L. P., "Exploratory Investigation of Vortex Bursting on the High-Angle-of-Attack Lateral Directional Stability Characteristics of Highly Swept Wings," AIAA Paper 80-0463, March 1980.

[10]Hummel, D., "Untersuchungen über das Aufplatzen der Wirbel an schlanken Delta Flügeln," *Z. f. Flugwissenschaften*, Vol. 13, Heft. 5, 1965, pp. 158–168.

[11]Hanff, E. S., and Huang, X. Z., "Roll-Induced Cross-Loads on a Delta Wing at High Incidence," AIAA Paper 91-3223, Sept. 1991.

[12]Hanff, E. S., and Ericsson, L. E., "Multiple Roll Attractors of a Delta Wing at High Incidence," Paper 31, AGARD-CP-494, July 1991.

[13]Ericsson, L. E., "Analysis of Wind-Tunnel Data Obtained in High-Rate Rolling Experiment with Slender Delta Wings," National Research Council (Canada), IAR-CR-14, Ottawa, Canada, Aug. 1991.

[14]Ericsson L. E., and Hanff, E. S., "Unique High-Alpha Roll Dynamics of a Sharp-Edged 65 Deg Delta Wing," AIAA Paper 92-0276, Jan. 1992.